JOURNAL OF AGRICULTURAL AND FOOD CHEMISTRY

Article

Cite This: J. Agric. Food Chem. XXXX, XXX, XXX−XXX

pubs.acs.org/JAFC

Metabolic Analysis Reveals Altered Long-Chain Fatty Acid Metabolism in the Host by Huanglongbing Disease

Joon Hyuk Suh,[†] Yue S. Niu,[§] Zhibin Wang,[‡,⊥] Frederick G. Gmitter, Jr.,[‡] and Yu Wang*[,†]

[†]Department of Food Science and Human Nutrition, Citrus Research and Education Center and [‡]Department of Horticultural Sciences, Citrus Research and Education Center, University of Florida, 700 Experiment Station Road, Lake Alfred, Florida 33850, United States

[§]Department of Mathematics, University of Arizona, 617 North Santa Rita Avenue, Tucson, Arizona 85721, United States

[⊥]Department of Citrus Breeding, The Citrus Research Institute, Southwest University, 2# Tiansheng Rd, Beibei, Chongqing 400715, China

Supporting Information

ABSTRACT: *Candidatus* Liberibacter asiaticus (CLas) is the presumed causal agent of Huanglongbing, one of the most destructive diseases in citrus. However, the lipid metabolism component of host response to this pathogen has not been investigated well. Here, metabolic profiling of a variety of long-chain fatty acids and their oxidation products was first performed to elucidate altered host metabolic responses of disease. Fatty acid signals were found to decrease obviously in response to disease regardless of cultivar. Several lipid oxidation products strongly correlated with those fatty acids were also consistently reduced in the diseased group. Using a series of statistical methods and metabolic pathway mapping, we found significant markers contributing to the pathological symptoms and identified their internal relationships and metabolic network. Our findings suggest that the infection of CLas may cause the altered metabolism of long-chain fatty acids, possibly leading to manipulation of the host's defense derived from fatty acids.

KEYWORDS: *Huanglongbing, metabolomics, long-chain fatty acid, lipid oxidation product, citrus*

INTRODUCTION

Huanglongbing (HLB) is a devastating citrus disease that has had a strong impact on citrus production worldwide. HLB was first noticed in areas of Asia and Africa, and just over a decade ago, spread in Americas, such as Brazil in 2004 and the USA in 2005.[1,2] Typical symptoms include irregular, blotchy mottling and leaf chlorosis, followed by tree decline, leaf and premature fruit drop, and the decrease of fruit yield and quality. In the USA, HLB is particularly prevalent in Florida, causing significant economic losses to the citrus industry.[3] HLB is related to three species of the *Candidatus* Liberibacter genus: *Candidatus* Liberibacter asiaticus (CLas), *Candidatus* Liberibacter americanus (CLam), and *Candidatus* Liberibacter africanus (CLaf). In Florida and in many other countries, CLas has been recognized as the major pathogen, which is transmitted to the host by the citrus psyllid.[4] There are controversial theories about the origins of HLB, but CLas most likely infected citrus in the continent through the psyllid transferring the bacteria from indigenous rutaceous plants to the citrus. HLB is one of the most complex plant diseases, with interactions among pathogenic bacteria, vectors, hosts, and the environment, and is spreading rapidly due to lack of natural resistance of the hosts, making it a challenge for researchers.

Because of difficulties in culturing the pathogen and characterizing programmed cell death on leaves, the mechanism of the plant−microbe interaction elicited by CLas infection has not been well studied. Instead, many studies focused on differently expressed gene and enzymatic reactions in signaling pathways and molecular mechanisms of the host.[5−13] In the wake of genomic and proteomic work, with advances in emerging technologies for the metabolite level, several researchers have started to use metabolomics to examine host signals as a response to HLB.[14−17] The study of metabolomes, the end products of cellular signaling processes, has been regarded as an ideal tool to reveal fundamental responses of a biological system to pathogenic changes; by contrast, changes in gene and enzyme levels do not give direct information on how those alterations are linked to changes in biological function.[18,19] On the basis of this advantage, metabolic changes of sugars, amino acids, organic acids or volatile organic compounds (VOCs) to the disease were studied using untargeted metabolomics methods.[14−17,20]

However, altered biochemical pathways regarding fatty acid metabolism under HLB have not been well investigated, although in plants, fatty acids play pivotal roles in pathogen defense. In 2017, a metabolomics approach to study the disease was conducted based on carboxylic compound profile, but the method only covered five fatty acids.[21] The participation of long-chain fatty acids, such as 16- and 18-carbon fatty acids, in plant defense to modulate basal, systemic, and effector-triggered immunity was well reviewed.[22] For example, palmitoleic acid (C16:1) was found to directly inhibit pathogenic growth, enhancing the host resistance against biotic

Received: November 10, 2017
Revised: January 10, 2018
Accepted: January 12, 2018
Published: January 12, 2018

DOI: 10.1021/acs.jafc.7b05273
J. Agric. Food Chem. XXXX, XXX, XXX−XXX

stress.[23] Similar to arachidonic acid (C20:4) derivatives as important inflammatory mediators in humans, α-linolenic acid (C18:3), linoleic acid (C18:2), and their oxylipins are reported to be deeply involved in immune responses to microorganisms in plants.[24,25] This indicates that the deficiency in intracellular responses of fatty acids can give rise to the decline of immune function, possibly aggravating pathological progression. If this happens, it might play a role in pathogen strategies for halting host immune responses. Until now, there is no evidence supporting this hypothesis, and even fatty acid composition in the host is unclear. Meanwhile, lipid oxidation products widely existing in biological systems may contribute to understand fatty acid metabolism indirectly because they are derived from fatty acids via lipid peroxidation and are considered as free-radical damage indicators related to biotic stress.[26] Hence, the investigation of fatty acids and their oxidation products in the host will broaden our understanding of pathological mechanisms in HLB disease.

There is growing evidence that CLas alters host metabolism, function, and hormone signaling to obtain intended benefits such as avoidance of plant defense.[5,27−29] The evaluation of changes in a host's metabolites may reveal clues to the modified metabolic pathways. As previously mentioned, despite the importance of fatty acids in host defense, there is lack of information in fatty acid-related signals under the disease. In this respect, extensive analysis of fatty acids and their oxidation products can help to understand complex mechanisms between pathogens and host metabolism. Therefore, in this study, a comprehensive targeted metabolomics approach was used to investigate terminal downstream products, including a variety of long-chain fatty acids and lipid oxidation products, which are directly associated with CLas-induced pathogenesis (HLB). The metabolic profiles of control and infected citrus leaves from three different cultivars were compared and further integrated/interpreted to examine disease markers, their internal relationships, and related metabolic network.

MATERIALS AND METHODS

Plant Materials. Control and infected Hamlin orange (*Citrus sinensis* (L.) Osbeck), Ray Ruby grapefruit (*Citrus paradisi* Macf.), and Murcott mandarin (*Citrus reticulata* Blanco) trees grown in the University of Florida's Citrus Research and Education Center were used as plant materials in this study. All trees were planted in August of 2014, and samples were harvested in June of 2016 (around 2 years old). They were similar size (1−1.5 m tall) and started to bear fruits. The infected trees were naturally infected in the field, and the controls were thoroughly protected from infection under a citrus undercover production systems (CUPS), consisting of pole and cable frame architecture, covered with 50-mesh anti-insect screen. Both control and infected trees were exposed to the same natural environment (temperature, humidity, and other factors, etc.) and were irrigated and fertilized daily. Heat-treated infected trees (Murcott mandarin) received thermotherapy at 42 °C in a steam chamber for 48 h at least three months prior to sample collection.[30] Three biological replicates and three technical replicates (n = 9) were performed for control and infected groups in each cultivar (Hamlin orange, Ray Ruby grapefruit, and Murcott mandarin). Likewise, three biological replicates and three technical replicates (n = 9) were conducted for the heat-treated infected group. In total, 21 individual trees (nine for control, nine for infected, and three for heat-treated infected) were employed for this study. Ten leaves per tree were randomly collected from different positions and ages: mature leaf from the low, moderate-age leaf from the middle, and juvenile leaf from the top of the tree. They were immediately frozen in liquid nitrogen and stored at −80 °C until use.

Bacterial Identification. Quantitative real-time polymerase chain reaction (qPCR) analysis was performed for identification of CLas bacteria in infected samples. The qPCR was not used for the control samples because they were already checked by qPCR to make sure there was no infection according to the regulation of CUPS. DNA was extracted from midribs (about 100 mg) using DNeasy Plant Mini Kits (Qiagen, Valencia, CA, USA). DNA quality and quantity were evaluated using a NanoDrop 1000 spectrophotometer (Thermo Scientific, Waltham, MA, USA). The qPCR amplifications were conducted in a Stratagene Mx3005P system (Agilent Technologies, Santa Clara, CA, USA) with HLB primers and probe (HLBaspr) based on 16S rDNA sequences and positive internal control primers and probe (COXfpr). A detailed procedure was performed as described by Li et al.[31] The results were expressed as cycle threshold (C_t) values for diagnosis.

Targeted Metabolomics. *Long-Chain Fatty Acid Profiling.* One-hundred milligrams of ground leaves was mixed with 20 μL of 5% butylated hydroxytoluene methanol solution. The sample was extracted with 2 mL of 2:1 *tert*-butyl methyl ether (MTBE): methanol solution containing an internal standard (heneicosanoic acid, C21:0) by agitation for 30 min. After centrifugation (3500 rpm, 10 min, 4 °C), supernatant was dried under a stream of nitrogen gas and reconstituted with 1 mL of hexane. Fatty acids were derivatized to fatty acid methyl esters (FAMEs) according to a previous method with a slight modification.[32] Briefly, the esterification was performed by partitioning with 1 mL of 1 M potassium hydroxide methanol solution in 30 min. The supernatant (1 μL) was analyzed using gas chromatography−tandem mass spectrometry (GC−MS/MS, TSQ 8000, Thermo Fisher Scientific, San Jose, CA, USA) equipped with an electron impact (EI) ion source. The analytes were separated on an HP-88 fused silica capillary column (100 m × 0.25 mm, 0.20 μm film thickness, Agilent Technologies, Santa Clara, CA, USA). The split ratio was 20:1 with a 1.25 mL/min flow rate. The injector and transfer line temperature were set at 250 and 240 °C, respectively. The oven temperature followed a program of 100 °C for initial, a ramp of 10 °C/min to 170 °C, holding at 28 min, another ramp of 2 °C/min to 220 °C, and holding at 10 min. The mass spectrometer was operated with timed-selective reaction monitoring (SRM) to obtain high sensitivity and selectivity. The ion source temperature was 280 °C and EI energy was 70 eV. SRM transitions were optimized as follows: m/z 74 → 43 for palmitic acid (PA, C16:0), stearic acid (SA, C18:0), arachidic acid (AA, C20:0), palmitoleic acid (POA, C16:1), oleic acid (OA, C18:1), and vaccenic acid (VA, C18:1), m/z 81 → 79 for linoleic acid (LA, C18:2), and m/z 79 → 77 for α-linolenic acid (ALA, C18:3), γ-linolenic acid (GLA, C18:3), arachidonic acid (ARA, C20:4), eicosapentaenoic acid (EPA, 20:5), n-3 docosapentaenoic acid (n-3 DPA, C22:5), n-6 docosapentaenoic acid (n-6 DPA, C22:5), and docosahexaenoic acid (DHA, C22:6). The collision energy was optimized at 10 V for PA, SA, AA, POA, OA, VA, LA, ALA, GLA, and ARA, and 15 V for the others. The analytes were assigned by comparing retention times and SRM transitions with authentic standards. The quantification was performed using calibration curves composed by plotting peak area ratios of the analyte to the internal standard against analyte concentrations.

Lipid Oxidation Product Profiling. One-hundred milligrams of leaves, pretreated with 20 μL of 5% butylated hydroxytoluene methanol solution, was extracted with 2 mL of acetonitrile containing an internal standard (cyclohexanone-2,4-dinitrophenylhydrazone) by agitation for 30 min. After centrifugation (3500 rpm, 10 min, 4 °C), supernatant was derivatized with 1 mL of 5 mg/mL 2,4-dinitrophenylhydrazine (DNPH) solution at room temperature (25 °C) in the dark place for 1 h. The derivatized sample was dried, reconstituted with 300 μL of acetonitrile, and gently loaded onto a C18 solid phase extraction (SPE, 1 mL, 100 mg, Restek Corporation, Bellefonte, PA, USA) cartridge, which was prewashed with 500 μL of acetonitrile twice. The pass-through was collected in a tube. After elution with 200 μL of acetonitrile, the pass-through and elution solvent were combined together (~500 μL),[33] and a 2 μL aliquot was injected into liquid chromatography−tandem mass spectrometry (LC−MS/MS, TSQ Quantiva, Thermo Fisher Scientific, San Jose,

DOI: 10.1021/acs.jafc.7b05273
J. Agric. Food Chem. XXXX, XXX, XXX−XXX

CA, USA) system. The LC−MS/MS analysis was performed as described by our previous work.[34] Like fatty acid profiling, the analytes were assigned and quantified using authentic standards.

Data Processing and Statistics. The data processing from GC−MS/MS and LC−MS/MS analyses was performed using Xcalibur software (version 3.0, Thermo Fisher Scientific, San Jose, CA, USA). For statistics, the extensive statistical analysis was conducted with the limited number of processed samples. The statistical package MVSP (version 3.1, Kovach Computing Services, Pentraeth, Wales, UK) was used for principal component analysis (PCA) and unweighted pair group method with arithmetic mean (UPGMA) cluster analysis. PCA for the integrated data was designed by R software (version 3.3.2, R Foundation for Statistical Computing, Vienna, Austria), and the marginal test using unpaired *t* test (*p*-value below 0.05) was adopted as criteria for marker determination. The fold change was calculated on the log scale using Excel. The R software, with package CCA and mixOmics installed, was used to acquire the heatmap (Pearson correlation coefficient, $-1 <$ value $< +1$) and correlation circle plot (cutoff value, 0.65) based on regularized canonical correlation analysis (rCCA) between fatty acid and lipid oxidation product data. The metabolic pathway enrichment analysis was performed using MBRole (http://csbg.cnb.csic.es/mbrole2/index.php).[35,36] Lastly, for the pathway mapping, biosynthesis of unsaturated fatty acids (map01040) in KEGG pathway database (http://www.genome.jp/kegg/) was used as a reference.

RESULTS

HLB-Induced Metabolic Changes in Citrus Hosts. The HLB-affected leaves externally showed typical pathological symptoms such as yellow veins and asymmetrically displayed blotchy mottles, which was not observed in healthy controls (Figure 1). For the infected samples, the presence of CLas

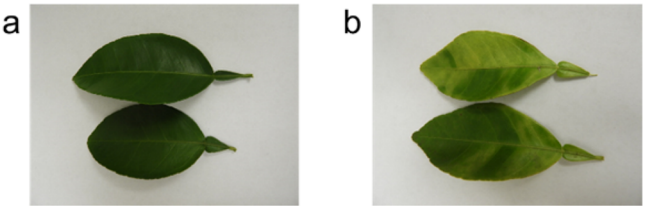

Figure 1. Photographic examples of (a) control and (b) HLB-affected leaves (Hamlin orange).

bacteria was confirmed by qPCR analysis.[31] Cycle threshold (C_t) values under 30 were considered confidently positive, and higher numbers were considered ambiguous.[37] The qPCR was not performed for the control samples because they were grown away from the disease in a strictly controlled environment (citrus undercover production systems (CUPS)) and were regularly checked by qPCR to make sure there was no infection. The qPCR results and general information on samples were presented in Table 1.

Metabolite profiles were examined in three different species of citrus including Hamlin orange (*Citrus sinensis* (L.) Osbeck), Ray Ruby grapefruit (*Citrus paradisi* Macf.), and Murcott mandarin (*Citrus reticulata* Blanco). Each cultivar included three control and three disease samples. Murcott mandarin had three additional samples from infected trees receiving thermal treatment,[30] which can decrease bacteria population levels and mitigate disease symptom (Table 1). A total of 46 metabolites (14 long-chain fatty acids and 32 lipid oxidation products) were selected as target compounds in a metabolomics approach. The fatty acids including palmitic acid (PA, C16:0), stearic acid (SA, C18:0), arachidic acid (AA, C20:0), palmitoleic acid (POA, C16:1), oleic acid (OA, C18:1), vaccenic acid (VA, C18:1), linoleic acid (LA, C18:2), α-linolenic acid (ALA, C18:3), γ-linolenic acid (GLA, C18:3), arachidonic acid (ARA, C20:4), eicosapentaenoic acid (EPA, 20:5), n-3 docosapentaenoic acid (n-3 DPA, C22:5), n-6 docosapentaenoic acid (n-6 DPA, C22:5), and docosahexaenoic acid (DHA, C22:6) were profiled using gas chromatography−tandem mass spectrometry (GC−MS/MS), and the lipid oxidation products were analyzed using liquid chromatography−tandem mass spectrometry (LC−MS/MS). All analytes were quantified with authentic standards, except in the case of malondialdehyde, by constructing calibration curves referenced to an internal standard. The results of absolute quantification are listed in Supplementary Tables 1 and 2.

Table 1. General Information of Citrus Leaf Samples and qPCR Results

cultivar	rootstock	sample code	C_t value[a]	status	group
Hamlin	Swingle	H/S-16		healthy	control
		H/S-18		healthy	control
		H/S-19		healthy	control
		H/S+13	27.82	HLB	infected
		H/S+15	26.70	HLB	infected
		H/S+24	26.91	HLB	infected
Ray Ruby	Sour orange	R/S-44		healthy	control
		R/S-45		healthy	control
		R/S-46		healthy	control
		R/S+1642	26.86	HLB	infected
		R/S+1741	28.68	HLB	infected
		R/S+1742	26.99	HLB	infected
Murcott	Kuharske	M/K-11		healthy	control
		M/K-12		healthy	control
		M/K-13		healthy	control
		M/K+36	38.79	ambiguous	heat-treated infected
		M/K+47	32.41	ambiguous	heat-treated infected
		M/K+8	38.00	ambiguous	heat-treated infected
		M/K+16	27.06	HLB	infected
		M/K+32	23.95	HLB	infected
		M/K+7	29.42	HLB	infected

[a] C_t value <30 (HLB positive).

First, principal component analysis (PCA) and cluster analysis were applied to individual cultivars based on fatty acid data. There were not many variables, but PCA clearly distinguished disease from control group on PC1 axes in each species (Supplementary Figure 1). Likewise, the cluster analysis separated samples into two major clusters according to the disease states (Supplementary Figure 2). Interestingly, the heat-treated infected samples looked similar to the controls rather than the infected samples, although they did not completely recover (there is no cure for HLB). The qPCR data (C_t value >30) supported their ambiguous conditions, evidence of reductions in bacterial titer (Table 1). Metabolic alterations in this group, making them closely resemble a normal state, would be a clue related to the disease (discussed later). Next, PCA was performed using integrated data from the three cultivars. Notably, regardless of cultivar, PCA based on fatty

DOI: 10.1021/acs.jafc.7b05273
J. Agric. Food Chem. XXXX, XXX, XXX−XXX

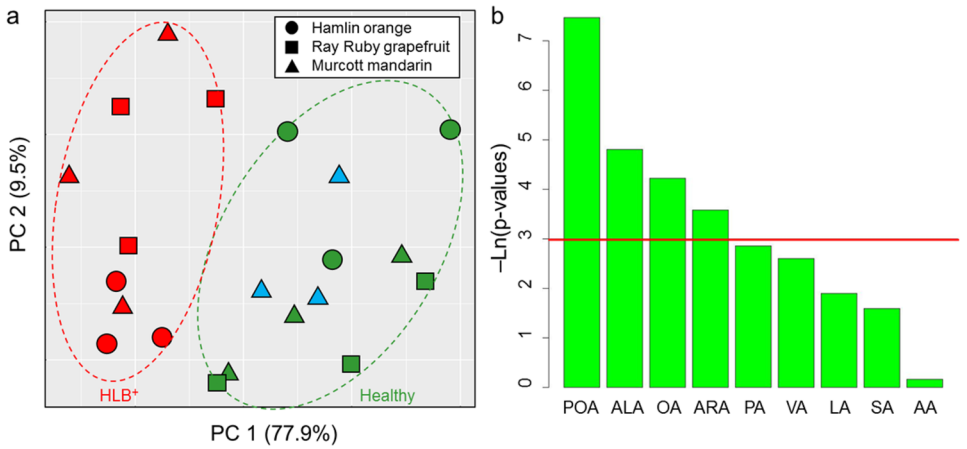

Figure 2. Metabolic difference of long-chain fatty acids between control and HLB-affected citrus leaves and their significance. (a) Score plot of principal component analysis for control (green), infected (red), and heat-treated infected (blue) groups. (b) Negative natural logarithm of *p*-value for fatty acids. Red line indicates *p*-value of 0.05.

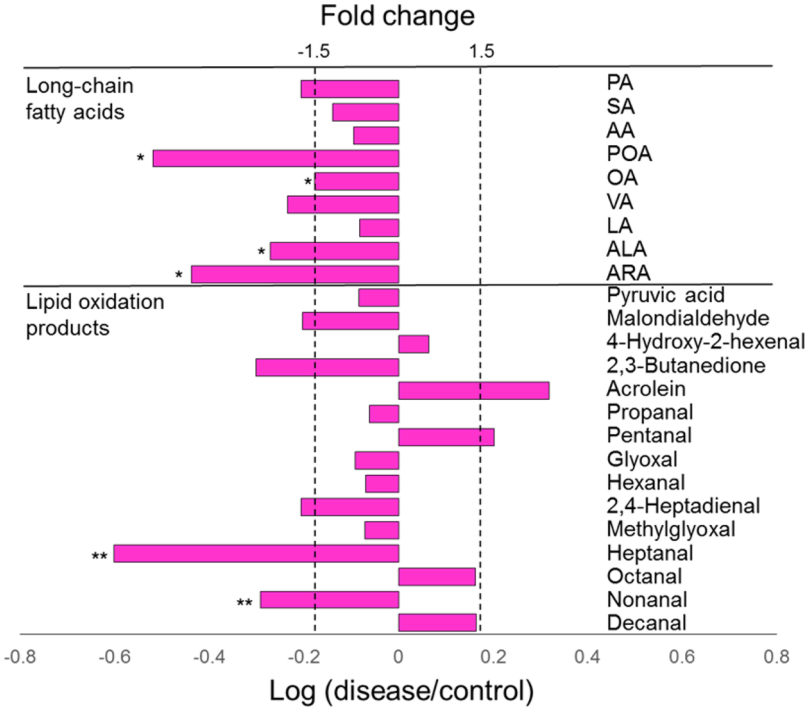

Figure 3. Fold changes of long-chain fatty acids and lipid oxidation products between control and infected groups. The graph shows metabolites with absolute fold changes larger than 1.2. Pivotal metabolites are marked with single (*p*-value < 0.05) and double asterisks (*p*-value < 0.001).

acid data again classified samples as "control" and "disease" except for the heat-treated group, explained by 87.4% on the first two principal components (PC1 and PC2) (Figure 2A). This indicated that metabolic changes of fatty acids were predominantly affected by the disease, not the cultivar. However, the results of PCA using lipid oxidation product data led to incomplete discrimination between two groups (Supplementary Figure 3A).

In the subsequent investigation, pivotal metabolic alterations related to the disease were identified using a marginal test. The metabolites with a *p*-value below 0.05 (−ln *p*-value > 3) were considered candidate markers. The criteria revealed that metabolites including four fatty acids (Figure 2B) and two lipid oxidation products (Supplementary Figure 3B) were reliably altered by the disease. A notable metabolic reduction was observed under disease: POA (−3.30-fold), ALA (−1.87-fold), OA (−1.51-fold), ARA (−2.75-fold), heptanal (−4.02-fold), and nonanal (−1.96-fold). Figure 3 shows metabolites with absolute fold changes larger than 1.2, including the markers.

Correlation between Long-Chain Fatty Acids and Lipid Oxidation Products. The relationship between long-chain fatty acids and lipid oxidation products was investigated using a heatmap and correlation circle plot. The heatmap based on the measurement of Pearson correlation coefficient (PCC) showed that heptanal and nonanal had positive correlations with fatty acids, especially with the markers including POA, OA, ALA, and ARA (Figure 4A). Concise heatmaps between these variables in three cultivars were presented in Figure 5. Although there was some weak correlation (<0.5) between heptanal and

DOI: 10.1021/acs.jafc.7b05273
J. Agric. Food Chem. XXXX, XXX, XXX−XXX

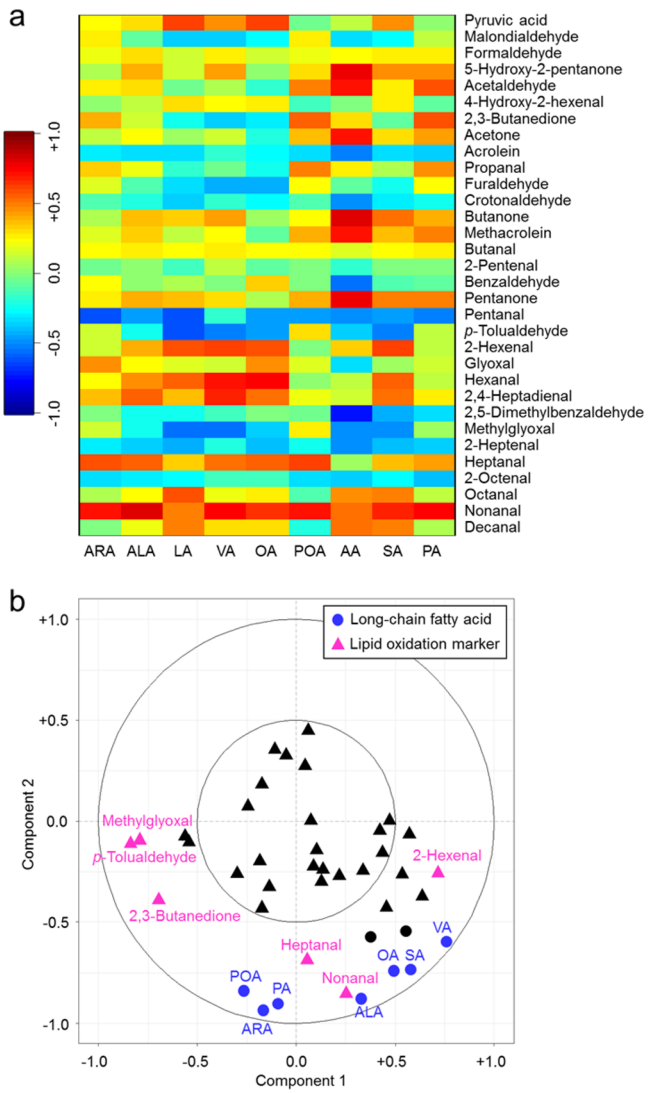

Figure 4. Correlation analysis of metabolic alterations between long-chain fatty acids and lipid oxidation products. (a) Heatmap displaying positive correlations (red) and negative correlations (blue) based on Pearson correlation coefficient. (b) Correlation circle plot obtained from regularized canonical correlation analysis. Fatty acids and lipid oxidation products that presented higher than the threshold (canonical correlation > 0.65) are colored in blue and pink, respectively.

fatty acids in Ray Ruby grapefruit, most relationships exhibited a positive correlation with high values, indicating the alterations occurred in the same direction for both fatty acids (POA, OA, ALA, and ARA) and lipid oxidation products (heptanal and nonanal). The highest coefficients were found in Murcott mandarin (>0.7). The relationship of these compounds was further visualized using the correlation circle plot based on regularized canonical correlation analysis (rCCA) with canonical correlation >0.65 and cosine angle >0 between variables (Figure 4B). In the plot, sharp angle reveals the correlation is positive, and a longer distance to the origin, the stronger relationship between variables. Heptanal and nonanal showed typical strong and positive correlation with the markers of fatty acids.

Metabolic Network Related to HLB. To identify possible metabolic pathways influenced by HLB, pathway enrichment analysis based on the target metabolites was performed (Table 2). Among candidate pathways, three metabolic pathways

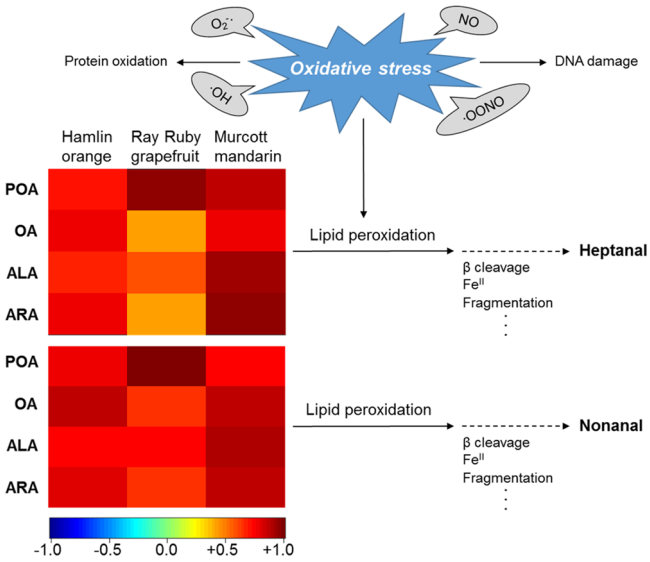

Figure 5. Relationship between metabolic responses of long-chain fatty acids and lipid oxidation products. Heatmaps displaying positive correlation between fatty acids (POA, OA, ALA, and ARA) and lipid oxidation products (heptanal and nonanal). Possible formation pathways of heptanal and nonanal are indicated by dotted lines. Red color represents equivalent alterations and blue color the opposite alterations.

Table 2. Results of Metabolic Pathway Enrichment Analysis

pathway	total matched (marker)[a]	*p*-value	FDR correction
biosynthesis of unsaturated fatty acids	11(3)	$2.00e^{-15}$	$3.00e^{-14}$
fatty acid biosynthesis	4(2)	$5.49e^{-06}$	$4.12e^{-05}$
linoleic acid metabolism	3(1)	$3.51e^{-05}$	$1.75e^{-04}$

[a]Pivotal metabolites with *p*-values below 0.05.

revealed high correlation with the metabolites, assigned by *p*-values (<0.05) and false discovery rate (FDR) values (<0.05). The pathways included (I) biosynthesis of unsaturated fatty acids, (II) fatty acid biosynthesis, and (III) linoleic acid metabolism. The most correlated pathway was pathway I, showing the highest matching score (36.7%) of matched/total metabolites including three marker fatty acids (ALA, OA, and ARA). Pathway I was also closely connected with the other candidate pathways: the end products (PA, POA, SA, and OA) of pathway II are substrates of pathway I, and the intermediate products (LA and ARA) of pathway I are used as starting and end products of pathway III. The network among these pathways is presented in Figure 6, and metabolite mapping on pathway I based on the integrated data from all cultivars is shown in Figure 7.

DISCUSSION

The HLB symptoms seen in citrus leaves, such as asymmetrical, blotchy mottling, and yellow veins (Figure 1), suggest that there might be some altered metabolic responses in the host. The PCA results shown in Figure 2A proved metabolic alterations in long-chain fatty acids. According to the metabolic differences, the diseased group was separate from the control group. The discrimination using PCA (unsupervised method) was satisfactory, so further separation using supervised methods (e.g., partial least-squares-discriminant analysis) was not

DOI: 10.1021/acs.jafc.7b05273
J. Agric. Food Chem. XXXX, XXX, XXX−XXX

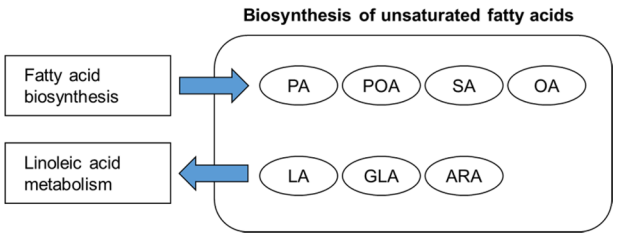

Figure 6. Metabolome network among biosynthesis of unsaturated fatty acids and other metabolic pathways based on the results of pathway enrichment analysis (p-value < 0.05).

needed. The results of PCA based on lipid oxidation products, however, showed less efficiency of group separation (Supplementary Figure 3A). This may be because some lipid oxidation products, such as glyoxal, can be generated from other sources (e.g., glucose) as well as fatty acids, making the whole mechanism complex.[38]

We found significant reduction of four fatty acids (POA, OA, ALA, and ARA) in the diseased group. They were confirmed as markers of fatty acids in disease detection (Figure 2B). Interestingly, levels of these fatty acids somewhat recovered after thermotherapy, as presented in Figure 8. The metabolic responses in the heat-treated group were comparable to those in the control group except for the case of OA. The influence of heat itself could be excluded since treatment was administered at least three months before collecting samples. This revealed the correlation between the fatty acid metabolism and disease progression. Among lipid oxidation products, heptanal and nonanal were found to decrease consistently in the disease group, which were proved as the markers of lipid oxidation products (Supplementary Figure 3B). However, the mechanism of their formation from fatty acids was obscure. Therefore, in the subsequent step, the relationship between these markers (heptanal and nonanal) and their parent fatty acids was investigated. As shown in Figure 4, heptanal and nonanal had a strong and positive correlation with fatty acids, especially with the marker fatty acids, compared to other products. The concise heatmap showing the correlation between marker groups in individual cultivars suggested that heptanal and nonanal would be derived from fatty acids including POA, OA, ALA, and ARA via lipid peroxidation (Figure 5). Several previous results support the proposed relationship,[39−41] indicating why heptanal and nonanal levels were reduced together with the decreased metabolic responses of fatty acids.

By investigating the metabolic network, three candidate pathways related to the disease were identified. Among the pathways, biosynthesis of unsaturated fatty acids (pathway I) was confirmed as the most relevant pathway (Table 2). The subsequent metabolite mapping on pathway I showed the metabolic changes of all fatty acids clearly, revealing their internal relationship (Figure 7). In the pathway, overall attenuated metabolic responses were observed, and notably, the level of a precursor (PA) to other fatty acids was found to decrease under disease. The PA level recovered after thermotherapy like other fatty acids (Supplementary Table 1). This indicated the altered precursor might affect metabolic changes in downstream fatty acids, including the pivotal fatty acids (POA, OA, ALA, and ARA).

Lack of metabolic responses in pathway I may aggravate host functional activities because long-chain fatty acids not only compose the physical barrier of plant cells, but also function as signal modulators regarding plant defenses to various stressors. A major plant fatty acid, ALA, is related to the production of reactive oxygen species (ROS) against pathogen invasion. It was reported that the defect of ALA formation in a mutant plant led to decreased ROS production after bacterial infection, showing increased susceptibility to the pathogens.[42] ALA is also

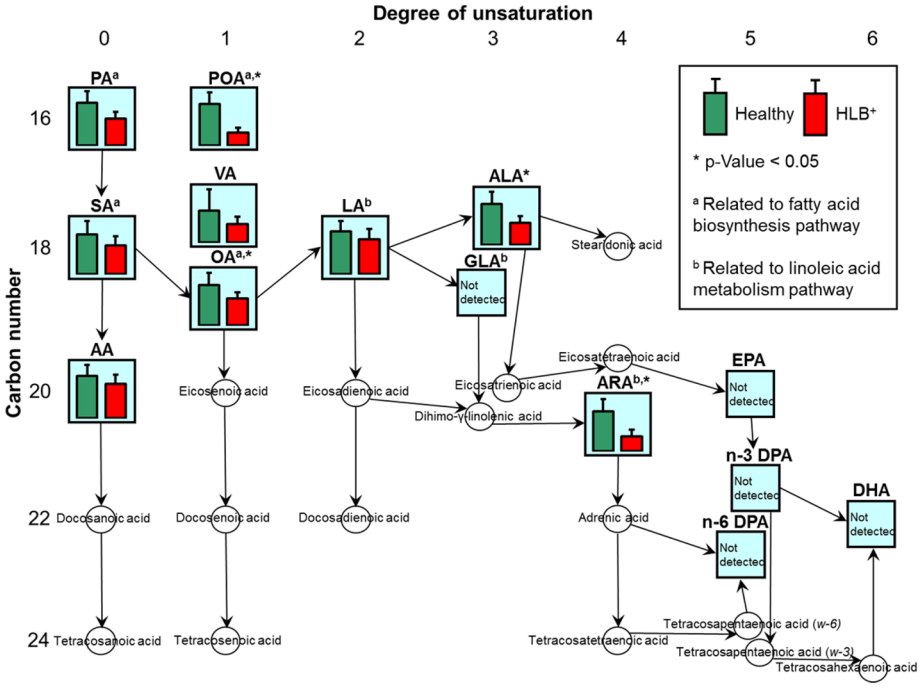

Figure 7. Metabolite mapping on the biosynthesis of unsaturated fatty acids pathway (pathway I). Bar graphs showed metabolite levels in control (green) and infected (red) leaves based on the integrated quantitative results (mean ± SD). Asterisks indicate p-value below 0.05. Metabolites related to other pathways as well as pathway I are marked with lowercase a and b (a, fatty acid biosynthesis; b, linoleic acid metabolism).

DOI: 10.1021/acs.jafc.7b05273
J. Agric. Food Chem. XXXX, XXX, XXX−XXX

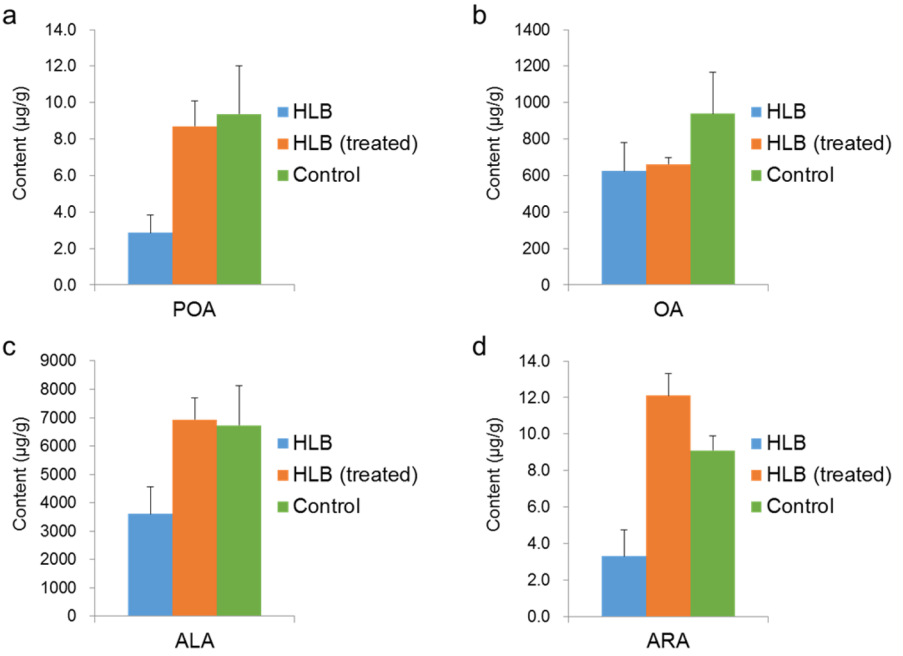

Figure 8. Metabolic responses of marker fatty acids in control, infected and heat-treated infected groups: (a) POA, (b) OA, (c) ALA, and (d) ARA.

a precursor of jasmonic acid (JA), a phytohormone involved in wound response to herbivory.[43] On the basis of our results, there could be two hypotheses for JA: one is that chronically reduced ALA due to disease may result in attenuated JA defense signaling, and the other, conversely, temporarily increased JA production may bring about the depletion of ALA. The latter is, however, unlikely because JA would be rapidly induced by psyllid attacks (HLB vector) during early infection stages,[44] and it is hard to explain alterations in other fatty acids, such as the precursor (PA) of ALA. The fatty acids including PA and OA are used as raw materials to synthesize cutin monomers, which constitute plant cuticles serving as a primary protective barrier against pathogens.[22,45] The depletion of cutin was reported to cause increased pathogen penetration through the cuticle layer.[46,47] Thus, if the supply of PA and OA is limited, cutin units would not be well organized, leading to deterioration of resistance capacity. POA and ARA are rarely studied because of their trace quantities, but there is growing evidence that they are involved in plant defense mechanisms. For example, POA was found to directly suppress pathogen growth in eggplants, enhancing the host resistance against biotic stress.[23] Plant-derived POA was also reported to show good antibacterial activity, as evidenced by its inhibitory effects on bacterial growth.[48] ARA-treated tomato leaves gave rise to reduced susceptibility to fungal infection.[49] As discussed above, a deficiency in long-chain fatty acids might affect the plant defensive system in various ways. Meanwhile, a study of sweet orange cultivars during maturation indicated that fatty acid profiles could change by fruit maturity, and especially, ALA was found to significantly increase over the entire extensive growing period.[50] This revealed that the depletion of ALA would impede maturation, probably correlating with major symptoms of HLB infection, such as small, asymmetrical leaves and early fruit drop.

There are several hypotheses that could explain why metabolic responses in pathway I were attenuated. The most probable explanation is that the bacteria (CLas) induce changes in the host's metabolism for their own benefits. It has already been suggested that CLas elicits a delayed defense response.[28] In addition, a salicylate hydroxylase encoded in the bacterial genome can lead to suppression of plant defense by converting salicylic acid into catechol, which has no effect inducing resistance.[29] Likewise, the long-chain fatty acids could possibly be changed for a similar purpose. For instance, if palmitoleic acid is reduced by pathogenesis, the host would be more vulnerable to bacterial infection. There might be another possibility that bacteria use host's metabolites as nutrients for their development. However, it was reported that CLas is unlikely to grow on fatty acids.[29] Thus, the depletion of fatty acids may result from bacterial strategies that manipulate the host's innate immune responses. Unfortunately, our results do not completely explain this phenomenon, but this poses an interesting question for future research.

In the present study, HLB disease was found to involve metabolic deficiency in the biosynthesis of unsaturated fatty acids pathway in citrus hosts. Our finding is newly reported here because previous metabolomics studies have usually focused on sugars, amino acids, organic acids, and their metabolism.[14−16,51,52] Furthermore, compared to the most recent work measuring five fatty acids,[21] this metabolomics approach covered a variety of long-chain fatty acids, including minor constituents, as well as their oxidation products, thereby leading to better understanding of fatty acid pathways related to the disease. With the help of various statistical models, we identified potential markers related to the disease, their internal relationship, and a related metabolic network. Although a pattern of metabolic change was consistently observed in different cultivars, further investigation using more samples (e.g., inoculated model) remains to be done. We believe this work will provide a new perspective and interpretation for understanding the complex pathology of HLB disease.

■ ASSOCIATED CONTENT

Supporting Information

The Supporting Information is available free of charge on the ACS Publications website at DOI: 10.1021/acs.jafc.7b05273.

DOI: 10.1021/acs.jafc.7b05273
J. Agric. Food Chem. XXXX, XXX, XXX−XXX

PCA score plots; cluster analysis diagrams; negative natural logarithm of *p*-values; quantification results (PDF)

AUTHOR INFORMATION

Corresponding Author

*E-mail: yu.wang@ufl.edu. Phone: +1-863-956-8673.

ORCID

Yu Wang: 0000-0002-2003-270X

Notes

The authors declare no competing financial interest.

ACKNOWLEDGMENTS

We thank Dr. Arnold W. Schumann and Laura Waldo (University of Florida/Citrus Research and Education Center) for providing all samples from model trees. We also thank Tony Trama (Florida Department of Citrus, FL, USA) for providing the GC−MS/MS instrument for the support of long-chain fatty acid profiling and thank Laura Reuss (University of Florida/Citrus Research and Education Center) for editing the manuscript.

ABBREVIATIONS USED

CLas, *Candidatus* Liberibacter asiaticus; HLB, Huanglongbing; qPCR, quantitative real-time polymerase chain reaction; C_t, cycle threshold; GC−MS/MS, gas chromatography−tandem mass spectrometry; LC−MS/MS, liquid chromatography−tandem mass spectrometry; SRM, selective reaction monitoring; PA, palmitic acid; SA, stearic acid; AA, arachidic acid; POA, palmitoleic acid; OA, oleic acid; VA, vaccenic acid; LA, linoleic acid; ALA, α-linolenic acid; GLA, γ-linolenic acid; ARA, arachidonic acid; EPA, eicosapentaenoic acid; n-3 DPA, n-3 docosapentaenoic acid; n-6 DPA, n-6 docosapentaenoic acid; DHA, docosahexaenoic acid; PCA, principal component analysis; rCCA, regularized canonical correlation analysis; FDR, false discovery rate

REFERENCES

(1) Texeira, D. C.; Ayres, J.; Kitajima, E. W.; Danet, L.; Jagoueix-Eveillard, S.; Saillard, C.; Bové, J. M. First report of a Huanglongbing-like disease of citrus in Sao Paulo state, Brazil and association of a new liberibacter species, "*Candidatus* Liberibacter americanus", with the disease. *Plant Dis.* **2005**, *89*, 107−107.

(2) Halbert, S. E. The discovery of Huanglongbing in Florida. *Proceedings of the 2nd International Citrus Canker and Huanglongbing Research Workshop 2005*: Orlando, Florida, USA, 2005; p 50.

(3) USDA. *Citrus: World Markets and Trade*; United States Department of Agriculture, 2016. http://usda.mannlib.cornell.edu/usda/fas/citruswm/2010s/2016/citruswm-01-20-2016.pdf (accessed October 15, 2017).

(4) Jagoueix, S.; Bove, J.-M.; Garnier, M. The phloem-limited bacterium of greening disease of citrus is a member of the α subdivision of the proteobacteria. *Int. J. Syst. Bacteriol.* **1994**, *44*, 379−386.

(5) Albrecht, U.; Bowman, K. D. Gene expression in *Citrus sinensis* (L.) Osbeck following infection with the bacterial pathogen *Candidatus* Liberibacter asiaticus causing Huanglongbing in Florida. *Plant Sci.* **2008**, *175*, 291−306.

(6) Nwugo, C. C.; Lin, H.; Duan, Y.; Civerolo, E. L. The effect of '*Candidatus* Liberibacter asiaticus' infection on the proteomic profiles and nutritional status of pre-symptomatic and symptomatic grapefruit (*Citrus paradisi*) plants. *BMC Plant Biol.* **2013**, *13*, 59.

(7) Zhao, H.; Sun, R.; Albrecht, U.; Padmanabhan, C.; Wang, A.; Coffey, M. D.; Girke, T.; Wang, Z.; Close, T. J.; Roose, M.; Yokomi, R. K.; Folimonova, S.; Vidalakis, G.; Rouse, R.; Bowman, K. D.; Jin, H. Small RNA profiling reveals phosphorus deficiency as a contributing factor in symptom expression for citrus Huanglongbing disease. *Mol. Plant* **2013**, *6*, 301−310.

(8) Fan, J.; Chen, C.; Brlansky, R. H.; Gmitter, F. G., Jr; Li, Z. G. Changes in carbohydrate metabolism in *Citrus sinensis* infected with '*Candidatus* Liberibacter asiaticus'. *Plant Pathol.* **2010**, *59*, 1037−1043.

(9) Fan, J.; Chen, C.; Yu, Q.; Brlansky, R. H.; Li, Z.-G.; Gmitter, F. G. Comparative iTRAQ proteome and transcriptome analyses of sweet orange infected by "*Candidatus* Liberibacter asiaticus. *Physiol. Plant.* **2011**, *143*, 235−245.

(10) Fan, J.; Chen, C.; Yu, Q.; Khalaf, A.; Achor, D. S.; Brlansky, R. H.; Moore, G. A.; Li, Z.-G.; Gmitter, F. G. Comparative transcriptional and anatomical analyses of tolerant rough lemon and susceptible sweet orange in response to '*Candidatus* Liberibacter asiaticus' infection. *Mol. Plant-Microbe Interact.* **2012**, *25*, 1396−1407.

(11) Aritua, V.; Achor, D.; Gmitter, F. G.; Albrigo, G.; Wang, N. Transcriptional and microscopic analyses of citrus stem and root responses to *Candidatus* Liberibacter asiaticus infection. *PLoS One* **2013**, *8*, e73742.

(12) Rawat, N.; Kiran, S. P.; Dongliang, D.; Gmitter, F. G., Jr; Zhanao, D. Comprehensive meta-analysis, co-expression, and miRNA nested network analysis identifies gene candidates in citrus against Huanglongbing disease. *BMC Plant Biol.* **2015**, *15*, 1−21.

(13) Du, D.; Rawat, N.; Deng, Z.; Gmitter, F. G., Jr Construction of citrus gene coexpression networks from microarray data using random matrix theory. *Hortic. Res.* **2015**, *2*, 15026.

(14) Slisz, A. M.; Breksa, A. P.; Mishchuk, D. O.; McCollum, G.; Slupsky, C. M. Metabolomic analysis of citrus infection by '*Candidatus* Liberibacter' reveals insight into pathogenicity. *J. Proteome Res.* **2012**, *11*, 4223−4230.

(15) Albrecht, U.; Fiehn, O.; Bowman, K. D. Metabolic variations in different citrus rootstock cultivars associated with different responses to Huanglongbing. *Plant Physiol. Biochem.* **2016**, *107*, 33−44.

(16) Freitas, D. d. S.; Carlos, E. F.; Gil, M. C. S. d. S.; Vieira, L. G. E.; Alcantara, G. B. NMR-based metabolomic analysis of Huanglongbing-asymptomatic and -symptomatic citrus trees. *J. Agric. Food Chem.* **2015**, *63*, 7582−7588.

(17) Killiny, N.; Valim, M. F.; Jones, S. E.; Omar, A. A.; Hijaz, F.; Gmitter, F. G., Jr; Grosser, J. W. Metabolically speaking: Possible reasons behind the tolerance of 'Sugar Belle' mandarin hybrid to Huanglongbing. *Plant Physiol. Biochem.* **2017**, *116*, 36−47.

(18) Fiehn, O. Metabolomics—The link between genotypes and phenotypes. In *Functional Genomics*; Town, C., Ed.; Springer: Dordrecht, Netherlands, 2002; pp 155−171.

(19) Fiehn, O.; Kopka, J.; Dormann, P.; Altmann, T.; Trethewey, R. N.; Willmitzer, L. Metabolite profiling for plant functional genomics. *Nat. Biotechnol.* **2000**, *18*, 1157−1161.

(20) Aksenov, A. A.; Pasamontes, A.; Peirano, D. J.; Zhao, W.; Dandekar, A. M.; Fiehn, O.; Ehsani, R.; Davis, C. E. Detection of Huanglongbing disease using differential mobility spectrometry. *Anal. Chem.* **2014**, *86*, 2481−2488.

(21) Killiny, N.; Nehela, Y. Metabolomic response to Huanglongbing: role of carboxylic compounds in citrus sinensis response to 'candidatus liberibacter asiaticus' and its vector, diaphorina citri. *Mol. Plant-Microbe Interact.* **2017**, *30*, 666−678.

(22) Kachroo, A.; Kachroo, P. Fatty acid−derived signals in plant defense. *Annu. Rev. Phytopathol.* **2009**, *47*, 153−176.

(23) Xing, J.; Chin, C.-K. Modification of fatty acids in eggplant affects its resistance to Verticilliumdahliae. *Physiol. Mol. Plant Pathol.* **2000**, *56*, 217−225.

(24) Prost, I.; Dhondt, S.; Rothe, G.; Vicente, J.; Rodriguez, M. J.; Kift, N.; Carbonne, F.; Griffiths, G.; Esquerré-Tugayé, M.-T.; Rosahl, S.; Castresana, C.; Hamberg, M.; Fournier, J. Evaluation of the antimicrobial activities of plant oxylipins supports their involvement in defense against pathogens. *Plant Physiol.* **2005**, *139*, 1902−1913.

(25) Alegria, T. G. P.; Meireles, D. A.; Cussiol, J. R. R.; Hugo, M.; Trujillo, M.; de Oliveira, M. A.; Miyamoto, S.; Queiroz, R. F.; Valadares, N. F.; Garratt, R. C.; Radi, R.; Di Mascio, P.; Augusto, O.;

DOI: 10.1021/acs.jafc.7b05273
J. Agric. Food Chem. XXXX, XXX, XXX−XXX

Netto, L. E. S. Ohr plays a central role in bacterial responses against fatty acid hydroperoxides and peroxynitrite. *Proc. Natl. Acad. Sci. U. S. A.* **2017**, *114*, E132−E141.
(26) Farmer, E. E.; Davoine, C. Reactive electrophile species. *Curr. Opin. Plant Biol.* **2007**, *10*, 380−386.
(27) Martinelli, F.; Uratsu, S. L.; Albrecht, U.; Reagan, R. L.; Phu, M. L.; Britton, M.; Buffalo, V.; Fass, J.; Leicht, E.; Zhao, W.; Lin, D.; D'Souza, R.; Davis, C. E.; Bowman, K. D.; Dandekar, A. M. Transcriptome profiling of citrus fruit response to Huanglongbing disease. *PLoS One* **2012**, *7*, e38039.
(28) Kim, J.-S.; Sagaram, U. S.; Burns, J. K.; Li, J.-L.; Wang, N. Response of sweet orange (*Citrus sinensis*) to '*Candidatus* Liberibacter asiaticus' infection: microscopy and microarray analyses. *Phytopathology* **2009**, *99*, 50−57.
(29) Wang, N.; Trivedi, P. Citrus Huanglongbing: a newly relevant disease presents unprecedented challenges. *Phytopathology* **2013**, *103*, 652−665.
(30) Hoffman, M. T.; Doud, M. S.; Williams, L.; Zhang, M.-Q.; Ding, F.; Stover, E.; Hall, D.; Zhang, S.; Jones, L.; Gooch, M.; Fleites, L.; Dixon, W.; Gabriel, D.; Duan, Y.-P. Heat treatment eliminates '*Candidatus* Liberibacter asiaticus' from infected citrus trees under controlled conditions. *Phytopathology* **2013**, *103*, 15−22.
(31) Li, W.; Hartung, J. S.; Levy, L. Quantitative real-time PCR for detection and identification of *Candidatus* Liberibacter species associated with citrus Huanglongbing. *J. Microbiol. Methods* **2006**, *66*, 104−115.
(32) Hung, W.-L.; Hsu, B.-Y.; Tung, Y.-C.; Ho, C.-T.; Hwang, L. S. Inhibitory effects of antioxidant vitamins against thiyl radical-induced trans fatty acid formation in PC-12 cells. *J. Funct. Foods* **2016**, *21*, 212−222.
(33) Matsui, K.; Sugimoto, K.; Kakumyan, P.; Khorobrykh, S. A.; Mano, J. I. Volatile oxylipins and related compounds formed under stress in plants. In *Lipidomics: Vol. 2: Methods and Protocols*; Armstrong, D., Ed.; Humana Press: Totowa, NJ, 2010; pp 17−28.
(34) Suh, J. H.; Ho, C.-T.; Wang, Y. Evaluation of carbonyl species in fish oil: An improved LC−MS/MS method. *Food Control* **2017**, *78*, 463−468.
(35) Chagoyen, M.; Pazos, F. MBRole: enrichment analysis of metabolomic data. *Bioinformatics* **2011**, *27*, 730−731.
(36) López-Ibáñez, J.; Pazos, F.; Chagoyen, M. MBROLE 2.0—functional enrichment of chemical compounds. *Nucleic Acids Res.* **2016**, *44*, W201−W204.
(37) Lee, J. A.; Halbert, S. E.; Dawson, W. O.; Robertson, C. J.; Keesling, J. E.; Singer, B. H. Asymptomatic spread of Huanglongbing and implications for disease control. *Proc. Natl. Acad. Sci. U. S. A.* **2015**, *112*, 7605−7610.
(38) Thornalley, P. J.; Langborg, A.; Minhas, H. S. Formation of glyoxal, methylglyoxal and 3-deoxyglucosone in the glycation of proteins by glucose. *Biochem. J.* **1999**, *344*, 109−116.
(39) Cao, J.; Deng, L.; Zhu, X.-M.; Fan, Y.; Hu, J.-N.; Li, J.; Deng, Z.-Y. Novel approach to evaluate the oxidation state of vegetable oils using characteristic oxidation indicators. *J. Agric. Food Chem.* **2014**, *62*, 12545−12552.
(40) Snyder, J. M.; Frankel, E. N.; Selke, E. Capillary gas chromatographic analyses of headspace volatiles from vegetable oils. *J. Am. Oil Chem. Soc.* **1985**, *62*, 1675−1679.
(41) Wang, Y.; Cui, P. Reactive carbonyl species derived from omega-3 and omega-6 fatty acids. *J. Agric. Food Chem.* **2015**, *63*, 6293−6296.
(42) Yaeno, T.; Matsuda, O.; Iba, K. Role of chloroplast trienoic fatty acids in plant disease defense responses. *Plant J.* **2004**, *40*, 931−941.
(43) Creelman, R. A.; Mullet, J. E. Jasmonic acid distribution and action in plants: regulation during development and response to biotic and abiotic stress. *Proc. Natl. Acad. Sci. U. S. A.* **1995**, *92*, 4114−4119.
(44) Dafoe, N. J.; Huffaker, A.; Vaughan, M. M.; Duehl, A. J.; Teal, P. E.; Schmelz, E. A. Rapidly induced chemical defenses in maize stems and their effects on short-term growth of *Ostrinia nubilalis*. *J. Chem. Ecol.* **2011**, *37*, 984−991.
(45) Pollard, M.; Beisson, F.; Li, Y.; Ohlrogge, J. B. Building lipid barriers: biosynthesis of cutin and suberin. *Trends Plant Sci.* **2008**, *13*, 236−246.
(46) Isaacson, T.; Kosma, D. K.; Matas, A. J.; Buda, G. J.; He, Y.; Yu, B.; Pravitasari, A.; Batteas, J. D.; Stark, R. E.; Jenks, M. A.; Rose, J. K. C. Cutin deficiency in the tomato fruit cuticle consistently affects resistance to microbial infection and biomechanical properties, but not transpirational water loss. *Plant J.* **2009**, *60*, 363−377.
(47) Buxdorf, K.; Rubinsky, G.; Barda, O.; Burdman, S.; Aharoni, A.; Levy, M. The transcription factor SlSHINE3 modulates defense responses in tomato plants. *Plant Mol. Biol.* **2014**, *84*, 37−47.
(48) Ruffell, S. E.; Müller, K. M.; McConkey, B. J. Comparative assessment of microalgal fatty acids as topical antibiotics. *J. Appl. Phycol.* **2016**, *28*, 1695−1704.
(49) Savchenko, T.; Walley, J. W.; Chehab, E. W.; Xiao, Y.; Kaspi, R.; Pye, M. F.; Mohamed, M. E.; Lazarus, C. M.; Bostock, R. M.; Dehesh, K. Arachidonic acid: an evolutionarily conserved signaling molecule modulates plant stress signaling networks. *Plant Cell* **2010**, *22*, 3193−3205.
(50) Nordby, H. E.; Nagy, S. Fatty acid profiles of three sweet orange cultivars during maturation. *J. Agric. Food Chem.* **1979**, *27*, 15−19.
(51) Chin, E. L.; Mishchuk, D. O.; Breksa, A. P.; Slupsky, C. M. Metabolite signature of *Candidatus* Liberibacter asiaticus infection in two citrus varieties. *J. Agric. Food Chem.* **2014**, *62*, 6585−6591.
(52) Hijaz, F. M.; Manthey, J. A.; Folimonova, S. Y.; Davis, C. L.; Jones, S. E.; Reyes-De-Corcuera, J. I. An HPLC-MS characterization of the changes in sweet orange leaf metabolite profile following infection by the bacterial pathogen *Candidatus* Liberibacter asiaticus. *PLoS One* **2013**, *8*, e79485.

DOI: 10.1021/acs.jafc.7b05273
J. Agric. Food Chem. XXXX, XXX, XXX−XXX